



Supporting Online Material for

Transgenic Inhibition of Synaptic Transmission Reveals Role of CA3 Output in Hippocampal Learning

Toshiaki Nakashiba, Jennie Z. Young, Thomas J. McHugh, Derek L. Buhl, Susumu Tonegawa*

*To whom correspondence should be addressed. E-mail: tonegawa@mit.edu

Published 24 January 2008 on *Science Express*
DOI: 10.1126/science.1151120

This PDF file includes:

Materials and Methods
SOM Text
Figs. S1 to S8
Tables S1 and S2
References

SUPPORTING ON-LINE MATERIALS

1. Materials and Methods

Generation of α CamKII-loxP-STOP-loxP-tTA (Tg2), TetO-TeTX (Tg3-TeTX) and TetO-GFP (Tg3-GFP) transgenic mice

For the Tg2 DNA construct, an Eco RI/Xba I fragment containing the tTA-coding sequence from the ptTA2 plasmid (Clontech) was ligated to a Xba I/Ase I fragment containing the β -globin polyadenylation (pA) signal isolated from the pBI plasmid (Clontech). This Ase I site was replaced with a Sal I site via a Sal I linker ligation. The loxP-STOP-loxP cassette was derived from a Not I/Eco RI fragment of the pBS302 plasmid (1). This cassette was modified by subcloning a 11.3 kb Xba I fragment isolated from a BAC clone containing the mouse NR1 gene locus (BACPAC Resource Center) into the Pst I site via linker ligation. This Eco RI/Not I (large) loxP-STOP-loxP fragment was then ligated to the Eco RI/Sal I fragment of the tTA-pA sequence, and finally ligated downstream of the Sal I/Not I fragment of the α -CamKII promoter from the pnn23 plasmid (2) to generate the final construct. For the Tg3-TeTX DNA construct, the TeTX light chain-coding sequence was PCR-amplified along with a Mlu I and Not I linker from the genomic sequence of *Clostridium tetani* (ATCC). The sequence coding for an N-terminal EGFP fusion was PCR-amplified from the pEGFP-N1 plasmid (Clontech) with a Sac II/Mlu I linker and the sequence for the C-terminal PEST sequence fusion was PCR-amplified from the pd1EGFPN-1 plasmid (Clontech) with a Not I/Xba I linker, then ligated to the TeTX light chain-coding sequence at the N- and C- terminus ends,

respectively. The resulting protein-coding sequence was subcloned into the Sac II and Xba I sites of the pTre2 plasmid (Clontech). The 22 kb Sal I fragment for Tg2 and the 4.0 kb Xho I/Sap I fragment for Tg3-TeTX were purified and individually injected to the pronuclei of fertilized eggs from C57BL/6 mice to generate transgenic offspring. For the Tg3-GFP line, the DNA construct was generated from the pBI-EGFP plasmid (Clontech) with minor modification. Each founder line was backcrossed with C57BL/6 mice and maintained in this genetic background.

Mouse breeding

The generation and characterization of the KA1-Cre transgenic mouse (Tg1) were previously described (3) and were maintained in C57BL/6 genetic background. After characterizing several founder lines by crossing with the α CamKII-tTA transgenic line (4) and immunostaining with a VAMP2 antibody, one of Tg3-TeTX lines was selected and crossed with the Tg1 to generate double transgenic mice heterozygous for both transgenes. In order to generate triple transgenic mice efficiently, heterozygous Tg1xTg3 (*KA1-Cre/+*, *TetO-TeTX/+*) mice were crossed each other to generate homozygous double transgenic mice (*KA1-Cre/KA1-Cre*, *TetO-TeTX/TetO-TeTX*). The male homozygous mice were then bred with female heterozygous Tg2 (*α CamKII-loxP-STOP-loxP-tTA /+*). A half of the progeny would be heterozygous triple transgenic mice (*KA1-Cre/+*, *TetO-TeTX/+*, *α CamKII-loxP-STOP-loxP-tTA /+*), which are referred to as CA3-TeTX mice. The other half of the progeny would be heterozygous double transgenic mice (*KA1-Cre/ +*, *TetO-TeTX/ +*, *+/+*), which would not express TeTX and therefore serve as control mice. Tg1xTg2xTg3-GFP mice were also generated in a similar way by using

Tg3-GFP mice instead of Tg3-TeTX mice during the breeding procedure. Tail DNA from all offsprings was genotyped by PCR to detect the presence of each transgene separately. PCR primers used are follows; For Tg1, 5'-AAATGGTTTCCCGCAGAACC-3' and 5'-CTAAGTGCCTTCTCTACACC-3'. For Tg2, 5'-CGCTGTGGGGCATTCTTACTTTAG-3' and 5'-GGGTCCATGGTGATACAAGG-3'. For Tg3-TeTX and Tg3-GFP, 5'-GTGGCGGATCTTGAAGTTCACC-3' and 5'-GACCCTGAAGTTCATCTGCACC-3'. The same PCR conditions (94°C for 2 min.; 94°C for 5 sec., 58°C for 1 min., 72°C for 1 min. x35 cycles; 72°C for 7 min.) were used for all primer pairs. For the genotyping of homozygous transgenic mice, a quantitative PCR was performed on tail DNA to determine the transgene copy number using probe-primer sets specific for the transgene (Tg1 or Tg3-TeTX) and SOD1 gene locus as internal control. PCR primers used were 5'-GCCGCGCGAGATATGG-3' and 5'-GCCACCAGCTTGCATGATC-3' for Tg1; 5'-CTGCTGCCCCGACAACCA-3' and 5'-TGTGATCGCGCTTCTCGTT-3' for Tg3-TeTX; 5'-TTTTTTTTCGCGGGTCCTTT-3' and 5'-ACCAGAGAGAGCAAGACGAGAAG-3' for SOD1. Probes used were 5'-CCAGCCAGCTATCAACTCGCGCC-3' for Tg1; 5'-CCCAGTCCGCCCTGAGCAAAGAC-3' for Tg3-TeTX; 5'-CTGCGGGCGCCTTCCGTCC-3' for SOD1. All procedures relating to animal care and treatment conformed to the Institutional and NIH guidelines.

Doxycycline (Dox) treatment

The minimum Dox concentration required to repress gene expression was determined by supplying drinking water with a varying dose of Dox to Tg1xTg2xTg3-GFP mice as well as to CA3-TeTX mice starting with the conception and ending in adulthood. Ten µg/ml

Dox (Sigma) supplemented with 1% sucrose (Sigma) was sufficient to repress GFP expression in Tg1xTg2xTg3-GFP mice as assessed by GFP antibody and TeTX expression in CA3-TeTX mice as assessed by VAMP2 antibody. When food containing 10 mg Dox per kg (Bioserve) was used, similar results were obtained with respect to GFP or TeTX expression. Therefore, we used Dox water (10 µg/ml) during the pregnancy and fostering periods and Dox food (10 mg/kg) after weaning to adulthood to keep TeTX in the repressed state. For a constitutive de-repression, the animals were kept on Dox-free water and Dox-free diet throughout their life.

Immunohistology

Mice were transcardially perfused with 4% paraformaldehyde (PFA) in 0.1 M sodium phosphate buffer (PB) and post-fixed by the same fixative overnight. For GFP and Netrin-G1 staining, the brains were further processed in 30% sucrose, embedded in OCT compound (SAKURA), and then frozen on the dry ice. Brain sections (50 µm thick) were prepared on a cryostat and collected in phosphate buffered saline (PBS). Free floating sections were first treated with 3% H₂O₂ in PBS for 10 minutes, followed by a treatment with 3% normal goat serum in TNB (TSA System, PerkinElmer) for 30 minutes. The sections were then incubated at 4°C overnight with primary antibodies diluted in same blocking solution (rat anti-GFP, 1/500, Nacalai USA Inc.; rabbit anti-Netrin-G1, 1/4000, ref. 5). After rinsing with TNT (100 mM Tris-HCl, 150 mM NaCl and 0.3 % Triton-X100), the sections were incubated with secondary antibodies (Alexa 488 conjugated anti-rat IgG, 1/200, Invitrogen; biotinylated anti-rabbit IgG, 1/500, Jackson ImmunoResearch) for 2 hours at room temperature, and then with streptavidin-

biotin/horseradish peroxidase complex (ABC complex, Vector) for 30 min. Netrin-G1 immunoreactivity was visualized by 7-min treatment with Cy3-tyramide (PerkinElmer) at room temperature. After rinsing with TNT, the sections were incubated with PBS containing DAPI (Invitrogen) and mounted on a glass slide. For VAMP2 immunostaining, brains were post-fixed overnight as above and sections (50 μ m thick) were prepared by vibratome. Primary antibody used here was rabbit anti-VAMP2 (1/250, Synaptic Systems) and VAMP2 immunoreactivity was visualized with Alexa 568-conjugated anti-rabbit IgG (1/200, Invitrogen). For VGLUT1 staining, cryostat sections (50 μ m thick) were incubated with primary antibody (guinea pig anti-VGLUT1, 1/1000, Chemicon) and then incubated with Alexa 488-conjugated anti-guinea pig IgG (1/200, Invitrogen). For GluR 1 staining, the sections were incubated with rabbit anti-GluR1 (1/40, Chemicon), then incubated with biotinylated anti-rabbit IgG, 1/500, Jackson ImmunoResearch). Signals were amplified with incubation with ABC complex (Vector), followed by visualization with fluorescein isothiocyanate (FITC) tyramide (PerkinElmer). For Tunel staining, the *in situ* cell death detection kit (Roche) was used following the manufacturer's instruction. As a positive control for DNA fragmentation, sections were treated with 10 units/ml DNase I (Promega) for 1 hour prior to Tunel staining. For the analysis of TA pathway projection, an anterograde tracer (Molecular Probes) was injected into medial entorhinal cortex. For this purpose, mice were deeply anesthetized with avertin and a 10% solution of biotinylated dextran amines (BDA-10,000) was injected at AP -3.60 mm and ML 4.70 mm from Bregma, and DV 1.70 mm to 2.40 mm from skull surface using a stereotaxic apparatus (0.3 μ l per injection). Five days after the injection, brains were fixed with 4% PFA in PB for 24 hours, then 50 μ m

coronal sections were made on a cryostat in the manner previously described. BDA was detected with FITC-tyramide following ABC complex incubation. Images were taken with a SPOT camera (Nikon).

In vitro electrophysiology

The experiments were conducted with male mice between 15 and 27 weeks of age. All the experiments were performed by operators blind to the genotypes and Dox treatments. Animals were euthanized by rapid cervical dislocation followed by decapitation. Their brains were quickly removed and immersed in ice-cold (4°C) artificial cerebral spinal fluid (ACSF) bubbled with a “carbogen” mixture of 95% O₂, 5% CO₂. The ionic composition of the ACSF was the same as in previous studies (6), consisting of (in mM): 119 NaCl, 2.5 KCl, 1.3 MgSO₄•7H₂O, 1.0 NaH₂PO₄•H₂O, 26.2 NaHCO₃, 2.5 CaCl₂, and 11.0 D-glucose (Mallinckrodt Chemicals, Hazelwood, MO). Brains were cooled for a brief (~2 min) period in ice-cold ACSF and then moved to a dissecting dish lined with filter paper and filled with ice-cold ACSF. The brain was then divided into hemispheres with sagittal cut down the midline. For each animal, transverse hippocampal slices for electrophysiological recordings were prepared from one hemisphere (chosen pseudo-randomly) while the remaining hemisphere was reserved for analysis of VAMP2 immunoreactivity. Hemispheres designated for immunohistology were placed in 4% PFA in PBS. In the hemisphere designated for electrophysiology, the hippocampus was dissected free and transverse slices (400 μm thickness) were cut on a manual tissue chopper (Stoelting, Wood Dale, IL). Hippocampal slices were then transferred onto a nylon mesh in an interface chamber used for recording (Fine Science Tools, Foster City,

CA) where they were maintained at 28°C and perfused with oxygenated ACSF (~1 ml/min). Investigation of the kinetics of Dox control over the blockade of synaptic transmission was carried out in the intact hippocampal slice preparation (Fig. S2). For all other experiments, clear isolation of the TA response required additional microdissection of the slices to remove the dentate gyrus and CA3 (7). Slices were allowed to recover for at least 45 min before microdissection, and given a total incubation time of 2.5 hr before experiments commenced. Electrophysiological analysis of synaptic transmission at SC and TA inputs was carried out concurrently in each hippocampal slice. Two bipolar stimulating electrodes (CE2C55, FHC, Bowdoin, ME), one placed in striatum radiatum (SR) and the other in striatum lacunosum-moleculare (SLM) of CA1 were used to stimulate the SC and TA pathways, respectively. fEPSPs were measured with a glass microelectrode (A-M Systems, Carlsborg, WA) filled with ACSF (electrical resistances: 4-7 M Ω) placed in SR of CA1. Evoked fEPSPs were amplified, digitized (Axoclamp-2B, DigiData 1320A Interface, Molecular Devices, Sunnyvale, CA), and analyzed using Axon Clampex 9.2 (Molecular Devices, Sunnyvale, CA). Stimuli were delivered to the TA and SC inputs with a 500 ms interval between stimulation through the two electrodes; TA stimulation evoked positive-going fields in SR while SC stimulation evoked negative-going fields in SR (7). SC and TA inputs were characterized by applying electrical stimulation (stimulus duration TA: 0.1 ms, SC: 0.08 ms) at a range of voltages (0.1 to 1.3 mV). Test stimuli were delivered four times per minute to provide one mean fEPSP measurement per minute. The initial slope of the fEPSP was plotted against the stimulation intensity to give an input-output relationship of the SC and TA pathways. Sample traces for SC and TA responses are representative of mean maximal fEPSP

slopes recorded at 1.3 mV. By the mid-way point of the range of stimulation intensities we applied, SC stimulation often induced CA1 population spikes (pSpikes) that were recorded as a positivity in the field potential (Table S1). As this phenomenon may be missing in CA3-TeTX mice, we used additional stimulation intensities (up to 2.0 mV) in looking for evidence of CA1 output. We also examined the efficacy of a high-frequency stimulation protocol (1 s train of 100 Hz tetanus) that significantly lowers the threshold for generating CA1 pSpikes (8) and reliably elicited pSpikes in control animals (89.5%; n = 19, N = 6). At the conclusion of each experiment, area CA1 and general slice viability was confirmed by antidromically eliciting CA1 pSpikes (recorded in stratum pyramidale) with alvear stimulation (Table S1). The values on the graphs represent mean fEPSP slopes \pm standard error of the mean. "N" represents number of animals; "n" indicates number of slices. Statistical analysis on input-output relations between treatment groups was carried out using two-way repeated-measures ANOVA (SPSS). Student's *t* test or ANOVA was used to compare mean fEPSP slopes elicited at the highest stimulation intensity if ANOVA analysis indicated a significant difference between groups ($p < 0.05$). Levene's test was done to determine equality of variances.

Morris water maze

The Morris water maze (MWM) task was conducted with male mice between 14 and 22 weeks of age, with minor modifications of the method described previously (9). All the experiments were performed by operators who were blind to the genotypes of the mice used and their Dox treatments. In brief, the mice were kept in a temperature-controlled room on a constant 12-hour light/dark cycle. The multiple experiments were conducted at

approximately the same time of the day. The mice were transported from the colony to a holding area where they sat undisturbed for 30 minutes prior to the experiment. The facility was in a rectangular dim-lit room (340cm x 297 cm) and consisted of a circular pool (160 cm diameter) filled with opaque water made with color paints (White 5130, Berghause; Peach 2906, Pearl Tempera) at 19 °C. Four large illuminated objects were hung as extramaze cues on each wall. A hidden circular platform (12 cm in diameter) was placed 1 cm below the water surface and the mice were trained to find the platform four trials per day for 10 days with an inter-trial interval of approximately 60 minutes. During training, the mice were released from four pseudorandomly assigned start locations (N, S, E, and W) and allowed to swim for 90 s. If a mouse did not find a platform within 90 s, it was manually guided to the platform and allowed to rest on the platform for 15 s. Probe trials were conducted on Day 6 and Day 11. The mice were released at the center of pool and were allowed to swim for 60 seconds in the absence of the platform. Data from the training session and probe trials were collected and analyzed with HVS Image Water 2020 software. An escape latency to the hidden platform was measured during training, and the quadrant occupancy as well as the number of crossing at the phantom platform location were measured during probe trials. These data were then averaged over mice of a particular genotype. Average position heat maps of water maze activity were created using Matlab (Mathworks Inc., Natick, MA). Position for each animal was broken down into 3 cm² bins and total time spent in those bins over a 60 second period was smoothed with a Gaussian function of a width of 5 cm. Smoothed position maps were then averaged across CA3-TeTX (n=10) and littermate controls (n=10). For visualization purposes,

maps were normalized to the maximum time spent out of all four maps combined (red: maximum time spent; blue: no time spent).

Contextual (CFC) and tone (TFC) fear conditioning

Fear conditioning was performed with male mice between 14 and 27 weeks of age in the animal facility during the light cycle with minor modifications of the method described previously (9). All the experiments were performed by operators who were blind to the genotypes and Dox treatments. Mice were transported from the colony to a holding room adjacent to the behavioral suite containing the fear conditioning chambers where they sat undisturbed for 30 minutes prior to the experiment. On Day 1, mice were brought into a room lit with dim red light and containing four conditioning chambers. The chambers had plexiglass fronts and backs and aluminum side walls with a curved plastic roof and measured 30 x 25 x 21 cm. The chamber floors consisted of 19 stainless steel rods spaced 16 mm apart connected via a cable harness to a shock generator. The chambers were cleaned prior to an introduction of an individual mouse into them with a quatricide and a solution of 1% acetic acid was placed beneath the chambers during the experiment to provide a dominant odor. Once placed in the chamber the mice were allowed to freely explore for 3 minutes, then received a single 1.25-mA footshock (2 s in duration) which co-terminated with a 30 seconds tone. Following the shock delivery, the mice remained in the chamber for 30 seconds, and then were returned to the home cages and transported back to the holding room. On Day 2, the mice were returned to the conditioning chambers under the conditions identical to those on Day 1 for a five minutes test. On Day 3, the mice were transferred to the second conditioning room adjacent to the first one.

This second room contained direct overhead fluorescent lighting and distinct chambers, measuring 30 x 25 x 21 cm, with plexiglass front and back walls, and aluminum side walls but with a flat roof. In addition, the floors of these chambers were made up with white plastic and the odor was provided with 0.25% benzaldehyde (in 100% ethanol). These lighting, chamber materials and odor employed on Day 3 provided a context quite distinct from that on Day 1. The mice were placed in this chamber for 3 minutes during which freezing responses were measured. This response compared to the response to the conditioning chamber on Day 2 gives a measure of the context specificity of contextual conditioning. The mice were then given the same tone as the one given on Day 1, but this time for 2 minutes and freezing responses were monitored. For Fig. 3G and H, a single group of mice were subjected successively to two CFC experiments each in a distinct chamber and under a distinct Dox condition (on-off or on-off-on). Under the on-off condition, mice which underwent 3 weeks of Dox withdrawal followed by 1 week of Dox re-administration were conditioned using the same protocol as that described above for Day 1. A subset of the CA3-TeTX mice under this Dox condition were subjected to immunohistology and slice physiology. They exhibited reductions in the VAMP2-IR (Fig. S7A and B) and the SC-CA1 fEPSP max (Fig. 2C) that were similar to those displayed by the CA3-TeTX mice which underwent 4 weeks of Dox withdrawal. The remaining mice were returned to the colony and received an additional 5 weeks of Dox diet (on-off-on condition). A subset of these mice were again sacrificed and subjected to immunohistology and slice physiology. The results showed restorations of VAMP2-IR and SC-CA1 fEPSP max (Fig. 2C). The remaining mice were placed in a second chamber (similar to the Day 3 chamber described above, except that the white plastic floor over

the stainless steel rods was removed to allow the delivery of a footshock) and were subjected to a second conditioning session using a protocol similar to that in the first conditioning session, except that the tone was omitted. Compared to the on-off experiment, in the on-off-on experiment, both genotypes demonstrated increased levels of preshock freezing. This is likely due to a generalization effect of freezing (10) during the 5 week-long Dox diet treatment. To allow comparison of the results of the two experiments, we subtracted this elevated pre-shock freezing from the freezing that occurred during the test session of the second experiment for both genotypes (Fig. 3G and H). For Fig. 3I and J, mice were first placed in the conditioning chamber for 3 consecutive days, 10 minutes per day. On Day 3, a single 1.25 mA footshock (2 s in duration) was delivered at 568 sec after being placed in the chamber, and the mice were allowed to stay in the chamber for an additional 30 s. On the next day, contextual memory was tested in same manner described above. Animals' activities in the chambers were recorded using FreezeFrame software. Freezing responses were assessed from the video images of the mice using FreezeView software, with a minimum bout time of 1 second. Freezing values were then averaged over mice of a particular genotype for each testing session.

Pre-exposure mediated contextual fear conditioning (PECFC)

This behavioral paradigm allows a test of pattern completion-based memory recall in CFC (11, 12). PECFC was conducted with male mice between 14 to 22 weeks of age in the animal facility during the light cycle. All the experiments were performed by operators who were blind to the genotypes of the mice used and their Dox treatments.

The mice were transported from the colony to a holding room where they sat undisturbed for 30 minutes prior to the experiment. On Day 1, mice were brought into the conditioning chamber which is same as the one described in the previous section, and allowed to explore freely for 10 min, and then transported back to their home cages. On Day 2, the mice were transported individually to the conditioning chamber and received a single 1.25 mA footshock (2 s duration) 10 seconds after being placed in the chamber. The mice remained in the chamber for a further 30 seconds, then were transported back to their home cages. On Day 3, contextual fear was assessed by placing the mice in the conditioning chamber for 5 minutes. For the Dox-on-off experiment shown in Fig. 3K, the mice were given pre-exposure sessions for 5 consecutive days, 10 minutes per day, and then Dox diet was replaced with the Dox-free diet. Four weeks later, the mice were transported individually to the conditioning chamber, and then received a single 1.25mA footshock (2 s duration) 10 seconds after being placed in the chamber. The mice remained in the chamber for a further 30 seconds, then were transported back to their home cages. On the next day, the mice were returned to the conditioning chambers for a five minutes test. During all these sessions, the animals' activity in the chamber was recorded using FreezeFrame software. Freezing behavior was assessed from the video image of the mouse using FreezeView software, with a minimum bout time of 1 second. Freezing values were then averaged over mice of a particular genotype for each session.

In vivo recording

Male mice (CA3-TeTX mice (N=9) and littermate controls (N=9), 18-22 weeks of age) were implanted with a microdrive array consisting of six independently adjustable

tetrodes (targeted to CA1: stereotaxic coordinates from bregma: 1.6 mm lateral; 1.8 mm posterior) as previously described (13). All experiments were conducted and analyzed by scientists blind to the genotypes of the animals. In the week following surgery the tetrodes were slowly lowered into CA1 as the mice were sitting quietly in a small high-walled enclosure (sleep box). Recordings began once stable unit recordings were obtained. On all three days of recording, sessions consisted of a "RUN" epoch on the track (10 laps) bracketed by 20 minute "SLEEP" sessions in which the animal rested quietly in the sleep box adjacent to the behavioral environment. On the initial day of recording (Day 1), the mice were placed at one end of a novel linear track (track dimensions: 80 cm long, 6 cm wide). Taking advantage of the tendency of the mice to spontaneously explore a novel space, animals were left free to run 10 laps on the track as extracellular action potentials were recorded. Position and directionality was tracked using a pair of infrared diodes placed 3 cm above the animals' head and 3 cm front to back. Diffuse room lighting was provided by low intensity spotlights focused onto four salient visual cues located on each of the walls of the recording chamber. This protocol was repeated twice, 24 hours (Day 2) and 48 hours (Day 3) following the initial exposure. At the conclusion of the experiment mice were given a lethal dose of anesthetic and a small electrical current (50 μ A) was run down each tetrode for 8 seconds to create a small lesion at the tip of the probe. Animals were then transcardially perfused with 4% PFA in PB and brains were removed. 50 μ m coronal slices prepared using a Vibrotome, mounted, and finally counterstained with Nuclear Fast Red to visualize electrode tracks and lesion sites. Recording position of each tetrode was verified by examining the location of the lesions under standard light microscopy.

Following data acquisition, action potentials were assigned to individual cells based on a spike's relative amplitudes across the four recording wires of a tetrode (9, 13).

Additionally, cells were classified as pyramidal units and included in the analysis if the following conditions were met: 1) a relatively broad waveforms ($> 350 \mu\text{s}$) 2) a peak firing rate greater than 5 Hz, and 3) a Complex Spike Index (a measure of bursting- see below) of greater than 5%. To remove firing occurring during times of immobility on the track, a velocity criterion of 2cm/sec was applied to limit analysis to period of motion. To characterize the consequences of trisynaptic input to CA1 on the activity of the CA1 pyramidal cells, we measured several properties including: 1) the Complex Spike Index (CSI)- defined as the percentage of spikes with first lag interspike intervals between 2 & 15 ms and whose second spike is smaller in amplitude than the first, 2) average and peak firing rates, 3) spike width (peak to trough), 4) place field size, expressed as the percent of sampled pixels in which the mean firing rate of the cell exceeded 0.5 Hz, and 5) spatial information (bits/spike, see below).

Statistical analysis

Results are given as mean \pm S.E.M. Where appropriate, statistical analyses were performed with analysis of variance (ANOVA) test. Otherwise, comparisons between groups were conducted using Student's *t* test. The null hypothesis was rejected at the $P < 0.05$ level.

2. Supporting Text

The DICE-K Method

The DICE-K method employs three transgenic mouse lines, Tg1, Tg2 and Tg3-TeTX that are crossed to heterozygosity for each transgene (Fig. 1B). In Tg1, the expression of Cre recombinase is driven by a transcriptional promoter with a tissue- or cell-type specificity. In Tg2, expression of the tetracycline transactivator (tTA), a transcriptional factor, depends on Cre-loxP recombination as well as a second transcriptional promoter that also exhibits a tissue- or cell-type specificity which overlaps with, but is different from, the specificity of the Tg1 promoter. In a Tg1xTg2 double transgenic line, tTA expression will take place only in the tissue or cell type in which both promoters are active (Fig. S1).

In Tg3-TeTX, the expression of TeTX is under the control of the Tet operator (Otet). In a Tg1xTg2xTg3-TeTX triple transgenic mouse, TeTX will be expressed only in those cells in which the tTA is expressed. The expression of TeTX can be blocked by a dietary supplement of doxycycline (Dox) which prevents tTA from binding to the Otet. Thus, when a mother pregnant with the triple transgenic mice is maintained on Dox diet during the pregnancy and subsequent fostering period, and the weaned mice are kept on the same diet until they grow to adulthood, TeTX expression will be repressed in these mice and hence the synaptic transmission will remain normal throughout the entire period (Dox-on or repressed state). When their diet is switched to one free of Dox, TeTX will be expressed only in those cells in which tTA is synthesized and consequently, synaptic transmission will be inhibited only at those synapses to which the tTA-positive cells

provide presynaptic terminals (Dox-on-off or de-repressed state). A subsequent switch back to Dox diet should restore synaptic transmission (Dox-on-off-on or re-repressed state).

The use of two tissue- or cell-type specific promoters with an overlapping specificity permits a greater spatial restriction of the genetic manipulation than a single promoter method. To demonstrate this, we crossed the KA1-Cre transgenic mouse (Tg1) (3) with the Cre-lox P recombination reporter mouse Rosa 26 (14) (single promoter system). We compared the pattern of β -galactosidase expression in the progeny mouse with that of the GFP in the Tg1xTg2xTg3-GFP mice (double promoter system). As shown in Fig. S1, β -galactosidase IR was detected strongly in CA3 and moderately in DG and facial nuclei. The IR was also detected, albeit at lower levels, in multiple other areas such as the anterodorsal thalamus, cerebellar granule cell layers, and vestibular nuclei. In contrast, GFP IR in Tg1xTg2xTg3-GFP mouse was detected only in CA3 and, to a lesser extent, in DG. Thus, if one makes a judicious choice of two promoters, one can expect a relatively tight spatial restriction of the genetic manipulation. Several genome-wide screening studies on the expression pattern of mouse genes in the brain (15-18) provide potential sources of promoters with some tissue- or cell-type specificities, although there remains a certain degree of trial and error in the identification of the specific transgenic line(s) which will allow a desired pattern of spatial restriction.

In the DICE-K method the temporal switch of synaptic blockade occurs on the time scale of a few weeks. We investigated the effect of the blockade of this time scale on the

general cytoarchitecture, distribution of synaptic markers, cell viability, and axonal projections in the hippocampus of CA3-TeTX mice that had undergone four weeks of Dox withdrawal. Fig. S3 and Fig. 1 show no indication of an alteration of the general cytoarchitecture. There also was no indication of abnormalities in the distribution of VGLUT1 IR (a presynaptic marker, Fig. S3, A and B) nor the GluR1 IR (a postsynaptic marker, Fig. S3, C and D), nor in the cell viability (Fig. S3, E and F). In order to examine the structural integrity of SC projections in the de-repressed CA3-TeTX mice, we crossed triple transgenic mice with the fourth transgenic mouse, Tg3-GFP (Fig. 1B) under Dox-on conditions and let the quadruple transgenic mice as well as triple transgenic CA3-GFP mice undergo four weeks of Dox withdrawal (de-repressed). The GFP IR shown in Fig. S3, G and H shows no discernable effect of the Dox withdrawal on the distribution of SC projections. Finally, we examined the integrity of TA projections in the de-repressed CA3-TeTX mice by injecting an anterograde tracer, biotinylated dextran amines (BDA-10,000), to the medial EC, and again found no indication of any abnormalities (Fig. S3, I and J). Thus, up to 4 weeks of blockade of synaptic transmission at the SC-CA1 and RC-CA3 synapses do not seem to result in nonspecific abnormalities in the cytoarchitecture of the hippocampus. These observations are supported by the report that synapse composition and organization are not affected by chronic blockade of synaptic activity by TeTX in cultured hippocampal neurons (19).

3. Supporting Figures

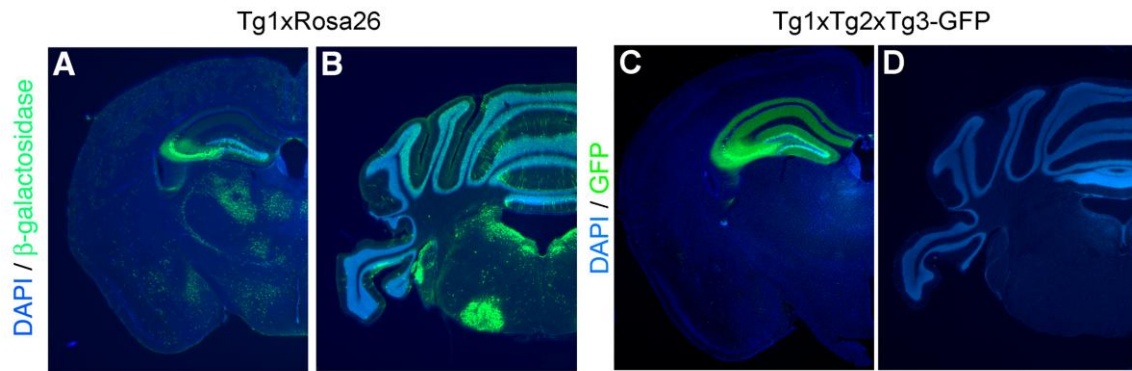


Fig. S1. Double promoter system confers tighter spatial restriction. (A and B) Immunofluorescence staining of coronal sections from a 12 week-old Tg1xROSA26 mouse (single promoter system) with antibodies specific for β -galactosidase (green) and cell nuclei marker, DAPI (blue). β -galactosidase is confined to cell somas. (C and D) Immunofluorescence staining of coronal sections of a 12 week-old Tg1xTg2xTg3-GFP mouse (double promoter system) with antibodies specific for GFP (green) and DAPI (blue). GFP spreads from somas to axons and dendrites.

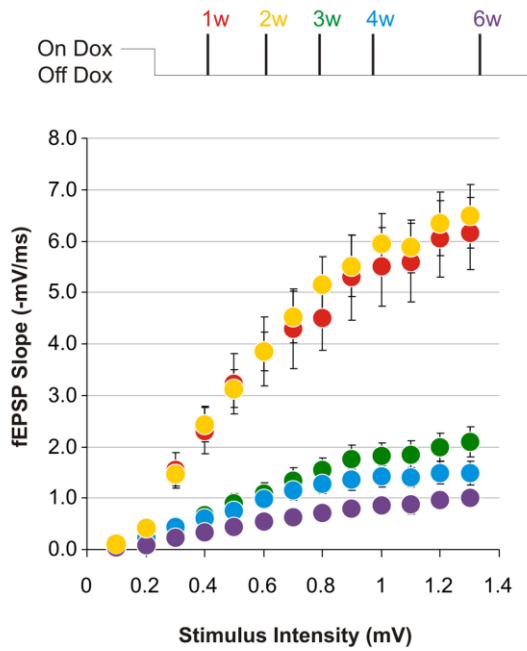


Fig. S2. Kinetics of Dox control over the blockade of synaptic transmission in CA3-TeTX mice. Input-output relationship of Schaffer collateral inputs to CA1 (stimulation range: 0.1 to 1.3 mV). CA3-TeTX mice were raised on Dox and then placed on a Dox-free diet for one (1w, red; N = 5, n = 11), two (2w, yellow; N = 6, n = 13), three (3w, green; N = 5, n = 16), four (4w, blue; N = 5, n = 15), or six weeks (6w, purple; N = 8, n = 14) prior to electrophysiological analysis.

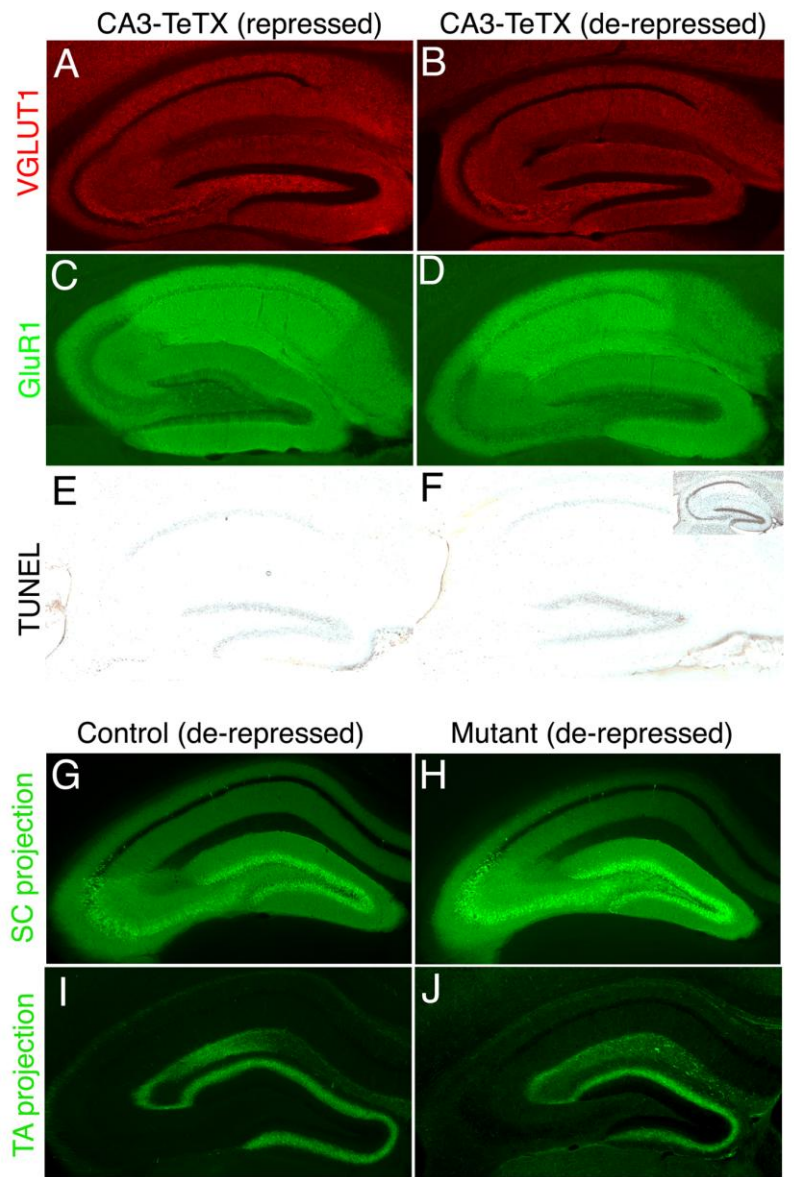


Fig. S3. Lack of molecular and cytoarchitectural abnormalities in de-repressed CA3-TeTX mice. (A, C and E) Sagittal sections from 16 week-old repressed CA3-TeTX mice. (B, D and F) Sagittal sections from 16 week-old de-repressed CA3-TeTX mice. (A and B) Staining with anti-VGLUT1 antibody (vesicular glutamate transporter 1, a presynaptic marker for glutamatergic nerve terminals). (C and D) Staining with anti-

GluR1 antibody (AMPA-type glutamate receptor 1, a postsynaptic marker). (**E** and **F**) TUNEL staining (marker for cell death). Insert in panel (**F**) is a positive control where the section was treated with DNaseI prior to TUNEL staining. (**G** to **J**) Axonal trajectories of SC and TA pathways. Immunofluorescence staining with an antibody specific for GFP (green) of coronal sections of a 16 week-old de-repressed CA3-GFP mouse (**G**) and a de-repressed quadruple Tg1xTg2xTg3-GFPxTg3-TeTX mouse (**H**). (**I** and **J**) Detection of an anterograde tracer injected into the medial entorhinal cortex of a 16 week-old de-repressed Tg1xTg3-TeTX control mouse (**I**) and de-repressed CA3-TeTX mouse (**J**).

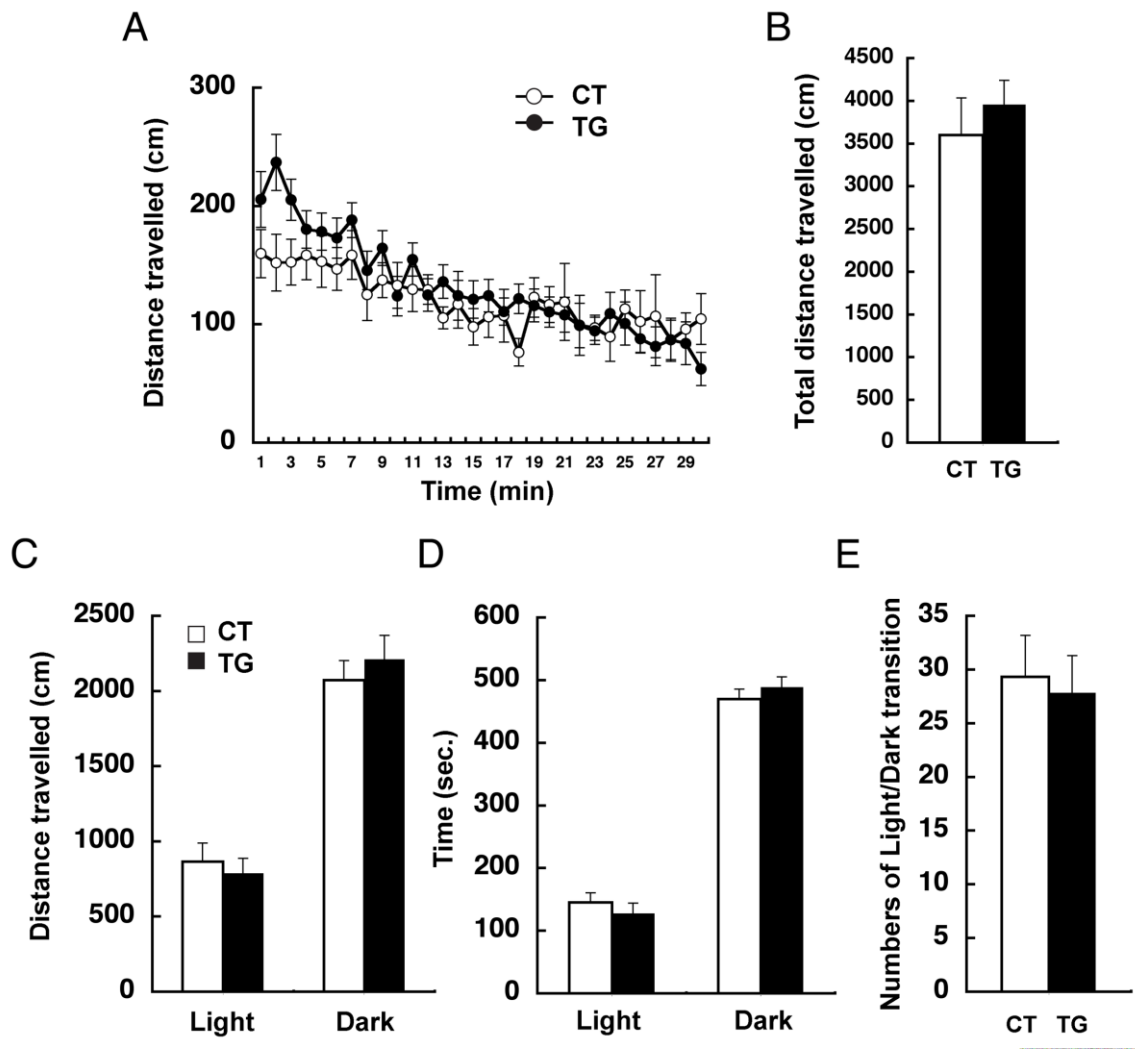


Fig. S4. CA3-TeTX mice exhibit no changes in the open field and light/dark transition tests. (A and B) Performance in an open field test of CA3-TeTX (TG, N=14) and their double transgenic control littermates (CT, N=12) that have undergone 4 weeks of Dox withdrawal (14-22 weeks of age). Total distance traveled in a novel open field chamber for a 30 minutes session is not significantly different between the two genotypes (TG, $39.6\text{m} \pm 2.8\text{m}$; CT, $36.0\text{m} \pm 4.4\text{m}$; $P > 0.05$). (C to E) Performance in a light/dark transition test for a 10 minute session of TG (N=13) and CT (N=13) that have undergone

4 weeks of Dox withdrawal (14-22 weeks of age). There was no significant difference between the two genotypes in the distance traveled in each compartment ($P > 0.05$) (**C**), the total time spent in each compartment ($P > 0.05$) (**D**) nor in the numbers of transition between the light and dark compartments ($P > 0.05$) (**E**).

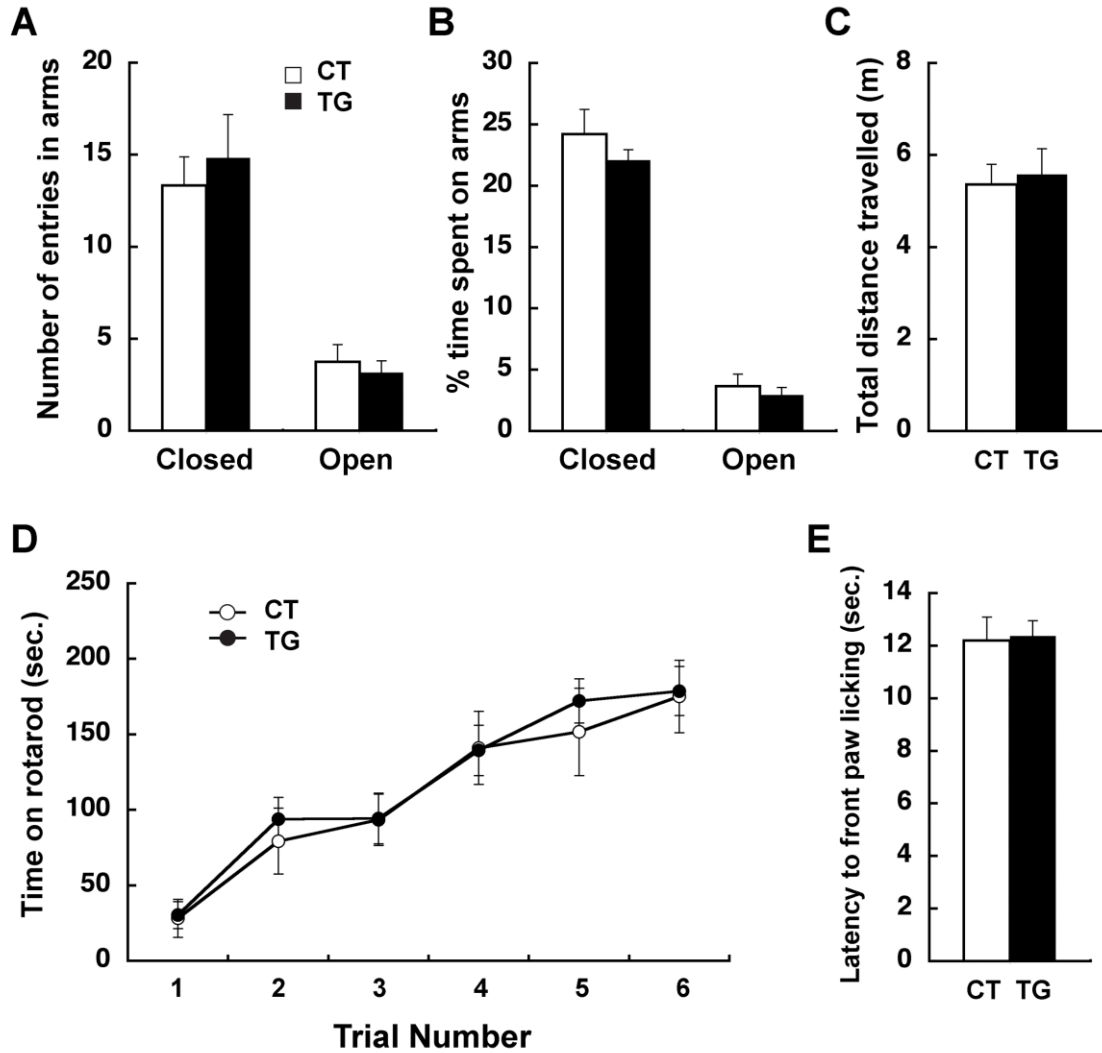


Fig. S5. CA3-TeTX mice exhibit no changes in elevated plus maze, rotarod and hot plate test. (A to C) Performance in the elevated plus maze task of CA3-TeTX (TG, N=12) and their double transgenic control littermates (CT, N=12) that have undergone 4 weeks of Dox withdrawal (14-22 weeks of age). There was no significant difference between the two genotypes in numbers of entries into open arms or closed arms ($P > 0.05$) (A), percentages of time spent in each type of arms ($P > 0.05$) (B) nor in the total distance traveled ($P > 0.05$) (C). (D) Performance in the rotarod test along six trials of

TG (N=17) and CT (N=13) that have undergone 4 weeks of Dox withdrawal (14-22 weeks of age). The performances of the two genotypes were not significantly different (2-way ANOVA: Genotype x Time $F(1,5) = 0.27$, $P = 0.93$; Time $F(1,5) = 42.42$, $P < 0.01$; Genotype $F(1,5) = 0.12$, $P = 0.73$). (E) Performance in a hot plate test of TG (N=12) and CT (N=12) that have undergone 4 weeks of Dox withdrawal (14-22 weeks of age). There was no significant difference on latency to lift their front paws ($P > 0.05$).

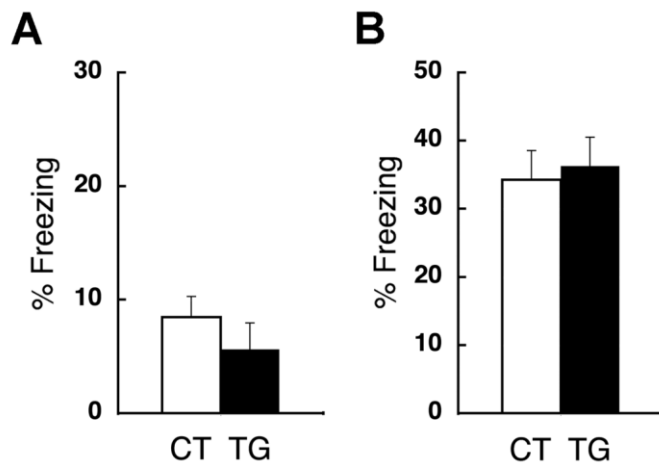


Fig. S6. Context specificity of CFC and freezing response in TFC (tone fear conditioning). (A) Context specificity of CFC of de-repressed CA3-TeTX (TG, N=25) and control littermates (CT, N=23) was tested by comparing the freezing levels in the conditioning chamber (Fig. 3F, measured 24 hours after the conditioning) and in a second and distinct chamber (measured 48 hours after the conditioning). Both genotypes exhibited less freezing in the second chamber compared to the first, indicating context specificity of CFC (TG, 14.6% ± 3.1% in the first chamber, 5.6% ± 2.3% in the second chamber, $P < 0.05$; CT, 25.9% ± 4.1% in the first chamber, 8.5% ± 1.8% in the second chamber, $P < 0.01$). The freezing responses in the second chamber were not different between the two genotypes (TG, 5.6% ± 2.3%; CT, 8.5% ± 1.8%; $P > 0.05$). (B) Tone-induced freezing in the second chamber was not different between the two genotypes (TG, 36.2% ± 4.3%; CT, 34.3% ± 4.3%; $P > 0.05$).

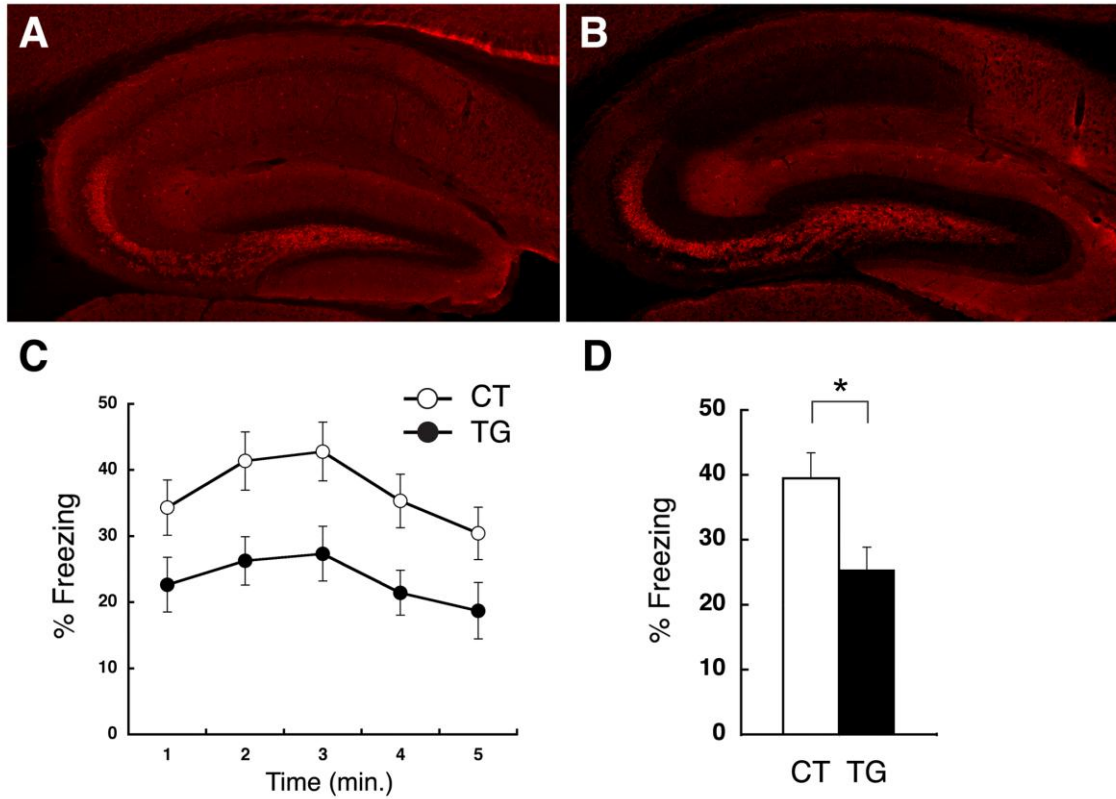


Fig. S7. VAMP2 immunoreactivity and contextual fear conditioning (CFC) in CA3-TeTX mice which underwent 3 weeks of Dox withdrawal followed by 1 week of Dox re-administration. (A and B) Immunofluorescence staining with a VAMP2 antibody of a hippocampal sagittal section from a 12 week-old CA3-TeTX mouse that has always been on Dox diet (A). The same staining of a section from a 16 week-old CA3-TeTX mouse that underwent 3 weeks of Dox withdrawal followed by 1 week of Dox re-administration (B). Note that the reduction of VAMP2-IR were similar to that displayed by the CA3-TeTX mice which underwent 4 weeks of Dox withdrawal (see Fig. 1K). (C and D) Performance in CFC in a novel context of CA3-TeTX mice (TG, N=28) and their double transgenic control littermates (CT, N=28) that underwent 3 weeks of Dox withdrawal followed by 1 week of Dox re-administration. (C) Kinetics of averaged freezing during the 5 minute test conducted 24 hours after conditioning. (D) Freezing

averaged over the first 3 minute test session for each genotype. Freezing responses across a 5 minute test in the conditioning chamber were significantly different between the two genotypes (2-way ANOVA: Genotype x Time $F(1,4) = 0.30$, $P = 0.88$; Time $F(1,4) = 6.66$, $P < 0.01$; Genotype $F(1,4) = 7.98$, $P = 0.007$). Average freezing responses during first three minutes in the conditioning chamber were significantly different between the two genotypes (TG, $25.4\% \pm 3.5\%$; CT, $39.5\% \pm 3.9\%$; $P < 0.05$).

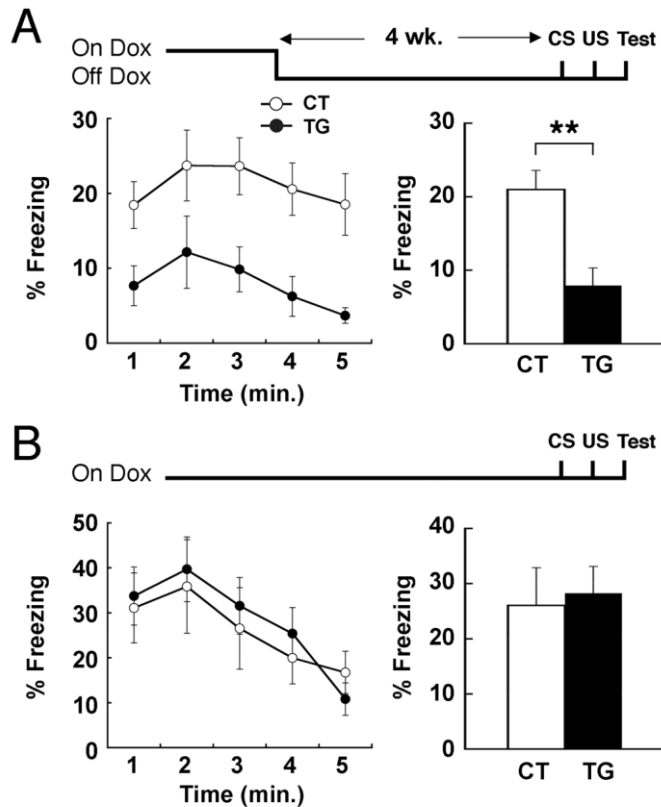


Fig. S8. Pre-exposure-mediated contextual fear conditioning (PECFC). Dox diet schedules, the minute to minute freezing response averaged over mice of a given genotype, and freezing responses averaged over the entire 5 min testing period are shown at top, on the left and right, respectively, in each panel. **(A)** Freezing responses of de-repressed CA3-TeTX mice (TG, N=20) and their control littermates (CT, N=20) were different. Minute to minute freezing; 2-way ANOVA: Genotype x Time $F(1,4) = 0.22, P = 0.93$; Time $F(1,4) = 2.19, P = 0.07$; Genotype $F(1,4) = 14.38, P = 0.0005$. Total freezing; TG, $7.9\% \pm 2.4\%$; CT, $21.0\% \pm 2.6\%$; $P < 0.01$. **(B)** Freezing responses of repressed CA3-TeTX mice (TG, N=12) and their control littermates (CT, N=12) were not different. Minute to

minute freezing; 2-way ANOVA: Genotype x Time $F(1,4) = 0.71$, $P = 0.59$; Time $F(1,4) = 11.16$, $P < 0.0001$; Genotype $F(1,4) = 0.08$, $P = 0.79$. Total freezing; TG, $28.2\% \pm 4.9\%$; CT, $26.0\% \pm 6.9\%$; $P > 0.05$.

4. Supporting Tables

| Measurement | Day 1 | | Day 2 | | Day 3 | |
|---------------------------------|----------------------------|-----------------------------|----------------------------|-----------------------------|----------------------------|-----------------------------|
| | Control (N = 9, n = 50) | CA3-TeTX (N = 9, n = 85) | Control (N = 9, n = 36) | CA3-TeTX (N = 8, n = 40) | Control (N = 9, n = 32) | CA3-TeTX (N = 7, n = 30) |
| Pyramidal cells | | | | | | |
| Mean firing rate (Hz) | 1.85 ± 0.15 | 2.64 ± 0.18* | 2.23 ± 0.28 | 1.81 ± 0.14‡ | 2.27 ± 0.23 | 1.77 ± 0.17 |
| Spike width (mS) | 548 ± 10.5 | 531 ± 9.39 | 559.9 ± 7.41 | 535 ± 8.46 | 558.6 ± 9.8 | 549 ± 11.2 |
| Complex spike index (bursting) | 22.27 ± 1.71 | 19.92 ± 1.15 | 21.23 ± 1.86 | 18.76 ± 1.55 | 21.96 ± 2.41 | 17.46 ± 1.55 |
| Peak rate (Hz) | 13.34 ± 1.69 | 13.26 ± 0.62 | 17.12 ± 1.41 | 12.41 ± 0.87 | 17.14 ± 1.3 | 11.32 ± 0.82 |
| Field size (% of sampled space) | 52.2 ± 2.81 | 69.32 ± 1.65* | 48.10 ± 2.8 | 56.53 ± 2.46*‡ | 44.36 ± 3.53 | 56.3 ± 2.68 * |
| Interneurons | | | | | | |
| Mean firing rate (Hz) | 17.34 ± 2.83 | 18.49 ± 3.09 | 16.09 ± 1.81 | 14.97 ± 2.68 | 15.99 ± 2.09 | 20.86 ± 3.53 |

* = Bonferroni post-test, $P < 0.001$, significantly different from control.

‡ = Bonferroni post-test, $P < 0.001$, significantly different from previous day.

Table S1. Properties of CA1 pyramidal cells and interneurons recorded *in vivo*.

| Measurement | Repression (On Dox) | | De-Repression (On-Off Dox 4 wk.) | | Re-Repression | | | |
|-------------------------------------|-----------------------------|--------------------------|-------------------------------------|--------------------------|------------------------------|--|--------------------------|--------------------------|
| | Control (N = 7) | CA3-TeTX (N = 10) | Control (N = 7) | CA3-TeTX (N = 5) | (On-Off Dox 3+1 wk.) | | (On-Off-On Dox 3+6 wk.) | |
| | | | | | Control (N = 6) | CA3-TeTX (N = 6) | Control (N = 6) | CA3-TeTX (N = 7) |
| SC fEPSP _{max} (-mV/ms) | 3.05 ± 0.27 (n = 18) | 3.45 ± 0.24 (n = 23) | 3.06 ± 0.23 (n = 23) | 0.50 ± 0.08* (n = 14) | 3.02 ± 0.30 (n = 20) | 0.80 ± 0.08 ^{†‡§} (n = 18) | 4.02 ± 0.46 (n = 15) | 3.65 ± 0.38 (n = 21) |
| | F(12,28) = 1.263, P = 0.293 | | F(12,24) = 11.201, P < 0.001 | | F(36,181) = 2.184, P < 0.001 | | | |
| I-O pSpikes (% slices) | 100 | 91.7 | 95.7 | 0 | 95.2 | 5.6 | 100 | 100 |
| Antidromic pSpikes (% slices) | 100 | 100 | 100 | 100 | 100 | 100 | 100 | 100 |
| TA fEPSP _{max} (mV/ms) | 0.11 ± 0.013 (n = 18) | 0.10 ± 0.011 (n = 23) | 0.09 ± 0.015 (n = 22) | 0.11 ± 0.015 (n = 13) | 0.09 ± 0.011 (n = 21) | 0.07 ± 0.008 (n = 19) | 0.10 ± 0.013 (n = 16) | 0.08 ± 0.011 (n = 19) |
| | F(12,28) = 1.156, P = 0.359 | | F(12,22) = 1.643, P = 0.151 | | F(36,175) = 0.798, P = 0.785 | | | |

All F and P values reflect two-way repeated-measures ANOVA on the interaction between genotype and stimulation intensities.
* = Student's *t*-test, *p* < 0.001, difference between Control and CA3-TeTX; Levene's test for equality of variances, equal variances not assumed
§ = Bonferroni post-test, *P* < 0.001, difference between CA3-TeTX (3+1 wk.) and Control (3+1 wk.)
‡ = Bonferroni post-test, *P* < 0.001, difference between CA3-TeTX (3+1 wk.) and Control (3+6 wk.)
† = Bonferroni post-test, *P* < 0.001, difference between CA3-TeTX (3+1 wk.) and CA3-TeTX (3+6 wk.)

Abbreviations:

Control Double transgenic control littermates (Tg1xTg3-TeTX)
CA3-TeTX Triple transgenic (Tg1xTg2xTg3-TeTX)
SC fEPSP_{max} Mean maximal fEPSP slope elicited by Schaffer collateral stimulation
I-O pSpikes CA1 population spikes recorded in stratum radiatum elicited by Schaffer collateral stimulation
Antidromic pSpikes CA1 population spikes recorded in stratum pyramidale elicited by antidromic stimulation of the alveus
TA fEPSP_{max} Mean maximal fEPSP slope elicited by temporoammonic stimulation

Table S2. *In vitro* electrophysiological characterization of specificity and reversibility of CA3-TeTX mice.

5. Statistics and Sample Sizes

Fig. 2, A to C. Please refer to Table S2 for a summary of all statistics and sample sizes relating to in vitro electrophysiology.

Fig. 3, A to D. Morris water maze task in the de-repressed CA3-TeTX (TG, N=10) and their control littermates (CT, N=10) mice.

Fig. 3A. The average escape latencies to the hidden platform location between the two genotypes were not significantly different (2-way ANOVA: Genotype x Day $F(1,9) = 0.86, P = 0.56$; Day $F(1,9) = 27.29, P < 0.0001$; Genotype $F(1,9) = 0.48, P = 0.50$).

Fig. 3B. Target quadrant occupancies were not significantly different between the two genotypes (TG, $33.6\% \pm 4.3\%$; CT, $33.4\% \pm 5.2\%$; $P > 0.05$ on Day 6; TG, $41.7\% \pm 4.6\%$; CT, $47.5\% \pm 5.2\%$; $P > 0.05$ on Day 11). Occupancies between target (TA) and opposite (OP) quadrants in TG were significantly different (TA, $33.6\% \pm 4.3\%$; OP, $20.3\% \pm 2.4\%$; $P < 0.05$ on Day 6; TA, $41.7\% \pm 4.6\%$; OP, $16.6\% \pm 2.9\%$; $P < 0.01$ on Day 11). Occupancies between target (TA) and opposite (OP) quadrants in CT were significantly different (TA, $33.4\% \pm 5.2\%$; OP, $19.6\% \pm 3.9\%$; $P < 0.05$ on Day 6; TA, $47.5\% \pm 5.2\%$; OP, $13.5\% \pm 2.9\%$; $P < 0.01$ on Day 11).

Fig. 3C. The number of platform crossings were not significantly different between the two genotypes (TG, 3.30 ± 0.63 ; CT, 3.70 ± 0.90 ; $P > 0.05$ on Day 6; TG, 5.60 ± 0.74 ; CT, 5.50 ± 0.72 ; $P > 0.05$ on Day 11).

Fig. 3, E and F. Contextual fear conditioning in a novel context of the de-repressed CA3-TeTX (TG, N=25) and their double transgenic control littermates (CT, N=23) mice.

Fig. 3E. Freezing responses across a 5 min test in the conditioning chamber were significantly different between the two genotypes (2-way ANOVA: Genotype x Time $F(1,4) = 0.39$, $P = 0.82$; Time $F(1,4) = 3.88$, $P < 0.01$; Genotype $F(1,4) = 4.36$, $P = 0.04$).

Fig. 3F. Total freezing responses during first three minutes in the conditioning chamber were significantly different between the two genotypes (TG, $14.6\% \pm 3.1\%$; CT, $25.9\% \pm 4.1\%$; $P < 0.05$).

Fig. 3, G and H. Contextual fear conditioning in a novel context of the CA3-TeTX (TG, N=28) and their double transgenic control littermates (CT, N=28) mice that have undergone 3 weeks of Dox withdrawal and subsequently 6 weeks of Dox reapplication.

Fig. 3G. Freezing responses across a five minutes test in the conditioning chamber were not significantly different between the two genotypes (2-way ANOVA: Genotype x Time $F(1,4) = 1.48$, $P = 0.21$; Time $F(1,4) = 7.88$, $P < 0.01$; Genotype $F(1,4) = 0.26$, $P = 0.61$).

Fig. 3H. Total freezing responses during first three minutes in the conditioning chamber were not significantly different between the two genotypes (TG, 43.56% \pm 3.1%; CT, 41.0% \pm 3.5%; $P > 0.05$).

Fig. 3, I and J. Contextual fear conditioning after 3 days familiarization (10 minutes per day) to a conditioning chamber of the de-repressed CA3-TeTX (TG, N=12) and their double transgenic control littermates (CT, N=12) mice.

Fig. 3I. Freezing responses across a five minutes test in the conditioning chamber were not significantly different between the two genotypes (2-way ANOVA: Genotype x Time $F(1,4) = 0.66$, $P = 0.62$; Time $F(1,4) = 1.54$, $P = 0.20$; Genotype $F(1,4) = 0.94$, $P = 0.34$).

Fig. 3J. Total freezing responses during first three minutes in the conditioning chamber were not significantly different between the two genotypes (TG, 24.9% \pm 6.0%; CT, 34.9% \pm 5.3%; $P > 0.05$).

Fig. 3K. Pre-exposure-mediated contextual fear conditioning (PECFC) task in the CA3-TeTX (TG, N=17) and their double transgenic control littermates (CT, N=15) mice. The mice were given pre-exposure sessions in the repressed state, and, four-weeks later, received a footshock in the de-repressed state. Freezing responses across a five minute test were significantly different between the two genotypes (2-way ANOVA: Genotype x Time $F(1,4) = 0.92$, $P = 0.46$; Time $F(1,4) = 3.47$, $P = 0.01$; Genotype $F(1,4) = 5.31$, $P =$

0.03). Total freezing responses between the two genotypes were significantly different (TG, $17.3\% \pm 3.4\%$; CT, $33.4\% \pm 6.7\%$; $P < 0.05$).

Fig. 4B. CA1 place field size, defined as percentage of space where the cell fires on the track, was significantly increased in CA3-TeTX (TG) mice on all days analyzed (2-way ANOVA: Genotype x Day $F(1,2) = 1.635$, $P = 0.197$; Genotype $F(1,2) = 32.816$, $P < 0.001$; Day $F(1,2) = 10.216$, $P < 0.001$). A significant decrease in place field size was observed in TG between Day 1 and Day 2 (Bonferroni post-test, $P < 0.001$), but not in their double transgenic control littermates. No significant changes were observed between Day 2 and Day 3 for either genotype.

Fig. 4C. Average firing rate of CA1 place cells was significantly higher in CA3-TeTX mice (TG) compared to their double transgenic control littermates (CT) on Day 1, but not on subsequent days (2-way ANOVA: Genotype x Day $F(1,2) = 6.96$, $P = 0.001$; Genotype $F(1,2) = 0.056$, $P = 0.814$; Day $F(1,2) = 0.93$, $P = 0.395$; Bonferroni post-test for Day 1, $P = 0.001$). A significant decrease in average firing rate was observed in TG between Day 1 and Day 2 (Bonferroni post-test, $P = 0.001$), but not in CT. No significant changes were observed between Day 2 and Day 3 for either genotype.

Fig. 4D. Spatial information, defined as bits/spike (see below), was significantly lower in CA3-TeTX (TG) mice on all days (2-way ANOVA: Genotype x Day $F(1,2) = 0.874$, $P = 0.418$; Genotype $F(1,2) = 71.62$, $P < 0.001$; Day $F(1,2) = 14.035$, $P < 0.001$). A significant increase in spatial information was observed in TG between Day 1 and Day 2

(Bonferroni post-test, $P < 0.001$), but not in their double transgenic control littermates. No significant changes were observed between Day 2 and Day 3 for either genotype.

Spatial information provided by each cell, was defined as:

$$I(R|X) \approx \sum_i p(\vec{x}_i) f(\vec{x}_i) \log_2 \left(\frac{f(\vec{x}_i)}{F} \right)$$

where $p(x_i)$ is the probability of the animal being at location x_i , $f(x_i)$ is the firing rate observed at x_i , and F is the overall firing rate of the cell (20). This equation yields bits/sec, to acquire bits/spike the output of this equation is then divided by the average firing rate F .

6. Supporting References

1. B. Sauer, *Methods Enzymol* **225**, 890 (1993).
2. J. Z. Tsien *et al.*, *Cell* **87**, 1317 (1996).
3. K. Nakazawa *et al.*, *Science* **297**, 211 (2002).
4. M. Mayford *et al.*, *Science* **274**, 1678 (1996).
5. T. Nakashiba, S. Nishimura, T. Ikeda, S. Itoharu, *Mech Dev* **111**, 47 (2002).
6. H. Kang *et al.*, *Cell* **106**, 771 (2001).
7. C. M. Colbert, W. B. Levy, *J Neurophysiol* **68**, 1 (1992).
8. K. G. Reymann *et al.*, *Brain Res Bull* **15**, 249 (1985).
9. T. J. McHugh *et al.*, *Science* **317**, 94 (2007).
10. B. J. Wiltgen, A. J. Silva, *Learn Mem* **14**, 313 (2007).
11. M. S. Fanselow, *Animal Learn Behav* **18**, 264 (1990).
12. J. W. Rudy, R. C. O'Reilly, *Behav Neurosci* **113**, 867 (1999).
13. T. J. McHugh, K. I. Blum, J. Z. Tsien, S. Tonegawa, M. A. Wilson, *Cell* **87**, 1339 (1996).
14. P. Soriano, *Nat Genet* **21**, 70 (Jan, 1999).
15. S. Gong *et al.*, *Nature* **425**, 917 (2003).
16. A. Visel, C. Thaller, G. Eichele, *Nucleic Acids Res* **32**, D552 (2004).
17. S. Magdaleno *et al.*, *PLoS Biol* **4**, e86 (2006).
18. E. S. Lein *et al.*, *Nature* **445**, 168 (2007)
19. K. J. Harms, A. M. Craig, *J Comp Neurol* **490**, 72 (2005).
20. W. E. Skaggs, B. L. McNaughton, K. Gothard, E. Markus, in *Advances in Neural Information Processing Systems*, S. Hanson, J. Cowan and C. Giles, Eds, (Morgan Kaufmann, San Mateo, 1993), vol. 5, pp. 1030-1037.